Mineralogical Magazine, April 1999, Vol. 63(2), pp. 179–187

High-resolution cathodoluminescence combined with SHRIMP ion probe measurements of detrital zircons

J. GÖTZE[1], U. KEMPE[1], D. HABERMANN[2], L. NASDALA[3], R. D. NEUSER[2] AND D. K. RICHTER[2]

[1] Freiberg University of Mining and Technology, Institute of Mineralogy, Brennhausgasse 14, D-09596 Freiberg, Germany
[2] Ruhr-University Bochum, Institute of Geology, Universitätsstraße 150, D-44780 Bochum, Germany
[3] Freiberg University of Mining and Technology, Institute of Theoretical Physics, B.-v.-Cotta Straße 4, D-09596 Freiberg, Germany

ABSTRACT

Cathodoluminescence (CL) microscopy and spectroscopy combined with SHRIMP ion probe measurements were carried out on detrital zircons from the Cretaceous Weferlingen quartz sand (Germany) to distinguish and characterize different zircon populations.

Investigations by CL microscopy, SEM-CL and BSE imaging show that there are three main types of zircons (general grain sizes of 100–200 μm): (1) apparently weakly zoned, rounded grains with relict cores, (2) well rounded fragments of optically more or less homogeneous zircon grains showing CL zoning predominantly parallel to the *z*-axis, and (3) idiomorphic to slightly rounded zircon grains typically showing oscillatory euhedral CL zoning. A fourth type of low abundance is characterized by well-rounded grain fragments with an irregular internal structure showing bright yellow CL.

High-resolution CL spectroscopic analyses reveal that blue CL is mainly caused by an intrinsic emission band centered near 430 nm. Dy^{3+} is the dominant activator element in all zircons, whereas Sm^{3+}, Tb^{3+}, Nd^{3+} have minor importance. Yellow CL (emission band between 500 and 700 nm) is probably caused by electron defects localized on the $[SiO_4]$ groups (e.g. related to oxygen vacancies) or activation by Yb^{2+} generated by radiation. Variations of the integral SEM-CL intensity are mainly controlled by the intensity of the broad bands and the Dy^{3+} peaks.

SHRIMP analysis provides *in situ* high-resolution U-Pb dating of single zircon grains and confirms different ages for the evaluated different zircon types. The measurements show that the U-Pb ages of the zircons from Weferlingen scatter over a wide range (340 to 1750 Ma), backing up earlier conclusions that the quartz sand from Weferlingen is quite heterogeneous in terms of provenance.

KEYWORDS: zircon, cathodoluminescence, SEM, SHRIMP, clastic sediment.

Introduction

ANALYSIS of accessory minerals has a long history of application to stratigraphic correlation and provenance evaluation in sedimentology. A large number of heavy minerals has been recorded from clastic sediments and many of these are source-diagnostic. Generally, the appearance of specific detrital minerals or characteristic associations can provide first fingerprints concerning source rocks and sedimentologic history, although the spectrum is often influenced and reduced by certain sedimentary and diagenetic processes. Therefore, genetic information obtained from the ultrastable minerals – zircon, rutile and tourmaline – is of special interest because of the chemical and mechanical resistivity and their common occurrence in clastic sediments. To get more information, classical methods of optical differentiation should be complemented by more sophisticated techniques such as single-grain analysis by microprobe, cathodoluminescence (CL) or radiometric dating. In the present study optical and spectral CL analysis combined with SHRIMP ion probe measurements were carried out on detrital zircons from the Cretaceous Weferlingen quartz sand (Germany) to decide: (1) whether or not CL provides useful differentiation of different zircon

types within a mixed detrital population, and (2) whether these evaluated zircon types are of different age and represent a different geological history. Furthermore, spectral CL measurements should provide more evidence about the causes of the different luminescence colours observed in zircon.

Materials and methods

The quartz sand deposit of Weferlingen is situated *c.* 45 km SE of Magdeburg in the Allertal graben zone (Fig. 1). The deposit consists of up to 200 m thick layers of Cretaceous (Lower Maastrichtian) estuarine and fluvial sands which were tilted by several NNE- and NW-striking faults. The quartz sand is well sorted and fine- to medium-grained (mean grain-size 0.26 mm). The mineralogical composition of the quartz sand is characterized by the predominance of quartz (>99%), the lack of feldspar, and only small concentrations of clay minerals and accessory heavy minerals (Götze, 1997).

Thirty sand samples were taken from the open mine near Weferlingen including samples from surface outcrops as well as material from a *c.* 50

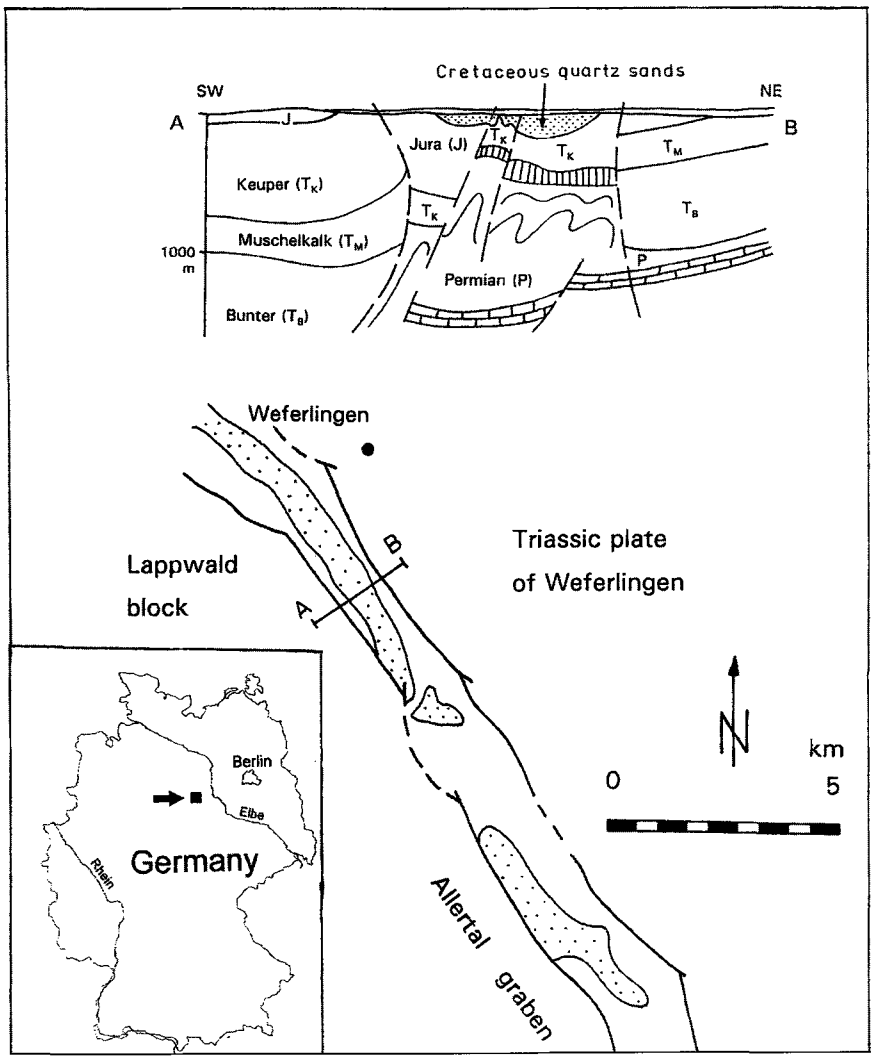

FIG. 1. Schematic map showing the geological position of the Cretaceous Weferlingen quartz sand.

m vertical profile through the upper sand suite. Heavy-mineral fractions of these samples were separated using heavy liquids and then analysed by polarizing microscopy. The zircon grains were evaluated for morphological characteristics, colour, transparency, and internal structures (e.g. zonation, inclusions). Representative aliquots of the characteristic zircon types were separated and polished thin sections of single zircon grains prepared.

Cathodoluminescence examinations of these samples were carried out on a 'hot cathode' CL microscope at 14 kV and with a current density of ~10 μA/mm^2. Luminescence images were captured 'on-line' during CL operations by means of an adapted digital video-camera (KAPPA 961-1138 CF 20 DXC with cooling stage). Cathodoluminescence spectra (spot diameter of *c.* 30 μm) were obtained using an EG&G digital triple-grating spectrograph with liquid nitrogen cooled, Si-based charge-coupled device (CCD) detector. The CCD camera was attached to the CL microscope by a 1.5 m silica-glass fibre guide (Neuser, *et al.*, 1995). Additionally, CL imaging by scanning electron microscopy (SEM-CL) and back-scattered electron (BSE) imaging (JEOL SEM with Oxford Mono-CL) were used to reveal detailed internal structures of zircon grains and to select suitable areas for SHRIMP analysis (i.e. areas that appeared to represent a specific type of internal structure on a scale of 20 μm). During SEM-CL the SEM was operated at 20 kV and a beam current of 0.6 nA.

Local analyses of the isotope composition of selected zircon grains (1–5 point analyses per grain) were performed using the SHRIMP II (Sensitive High Resolution Ion MicroProbe) at the Physical Department of the Curtin University of Technology, Perth, Western Australia. Eight masses (196Zr_2O, 2s; 204Pb, 10s; 206Pb, 10s; 207Pb, 50s; 208Pb, 10s; 238U, 5s, 248ThO, 5s; 254UO, 2s) and background (204.1, 10s) were measured in seven cycles after surface scanning. The focussed primary O_2 beam (10 kV and 3 nA) had a diameter of about 15 μm, which was confirmed by SEM measurements. Unknowns were measured versus the Curtin standard CZ3 (cf. Pidgeon *et al.*, 1994; Smith *et al.*, 1998). The standard values used are taken from Jaffey *et al.* (1971) and the 204 Pb correction for common lead follows Compston *et al.* (1984).

Results and discussion

The heavy mineral assemblage of the Weferlingen quartz sand consists mainly of zircon, tourmaline, rutile, andalusite, and opaque minerals (mainly ilmenite; Fig. 2). The predominance of the stable heavy minerals and the high roundness of most

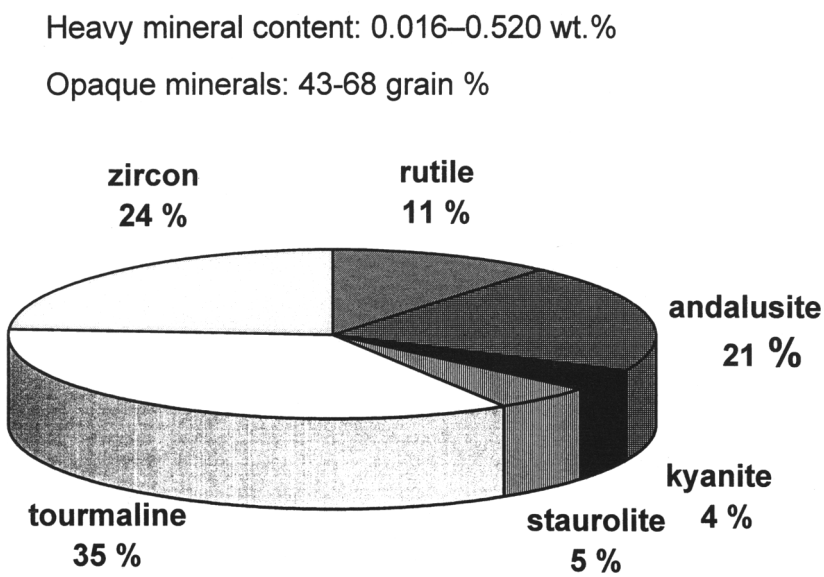

FIG. 2. Average composition of the heavy-mineral assemblage in the Weferlingen quartz sand.

grains illustrate the high maturity of the sand probably resulting from reworking of previously existing sedimentary source rocks. Different morphological types of zircons indicate the existence of more than one source. Therefore, a sophisticated examination of the zircons should provide more evidence about different detrital zircon populations.

Investigations by optical and CL microscopy, SEM-CL and BSE imaging revealed that there are three main types of zircons and a fourth type of low abundance:

(1) apparently weakly zoned, rounded grains (average grain size ~200 μm) with relict cores of about 100 μm (Plate 7A);

(2) rounded fragments (100–200 μm) of optically more or less homogeneous zircon grains showing CL zoning predominantly parallel to the *z*-axis (Plate 7B);

(3) idiomorphic to slightly rounded, about 200 μm long zircon grains typically showing oscillatory, euhedral concentric CL zoning (probably igneous origin, Plate 7C).

(4) A fourth type is characterized by well-rounded grains (~100 μm in diameter) with an irregular internal structure under CL (Plate 7D). Only several grains of this type were detected.

Generally, CL and BSE imaging reveal the same internal structures but with inverse intensity relations (Plate 7A–D). Only type 2 zircons show no internal structures in BSE image.

The investigations by CL microscopy show that the different zircon types significantly differ in CL colour (Plate 7). Type 1 zircons exhibit a bright blue luminescent core, whereas the outer rim luminescence is only dull. Type 2 zircons show alternations of blue and yellow luminescing zones orientated parallel to the *z*-axis. Microcracks within the zircon grains, which are also orientated parallel to the z-axis (compare Plate 7B, BSE image), cause bright yellow CL. Type 3 zircons are characterized by deep blue CL with CL zoning due to varying CL intensity. A bright yellow CL with irregular distribution is characteristic for zircons belonging to type 4.

CL spectroscopy provides detailed information about the origin of these different CL colours and incorporation of activator elements in zircon (Figs. 3–6). High-resolution spectroscopic analyses of the CL emission reveal that Dy^{3+} is the dominant activator element in all zircons (especially those showing blue CL), whereas other *REE* such as Sm^{3+}, Tb^{3+}, Nd^{3+} have minor importance (Fig. 4). The peaks at *c.* 485 nm

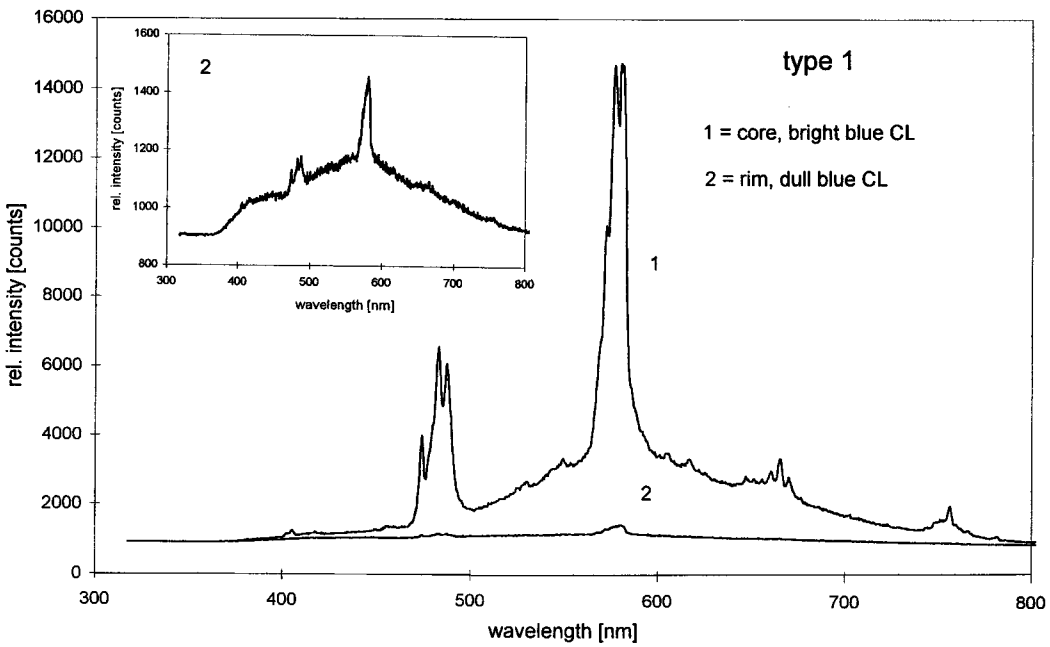

FIG. 3. CL emission spectra of core (1) and rim (2 and inset) of the investigated type 1 zircon (see Plate 7A).

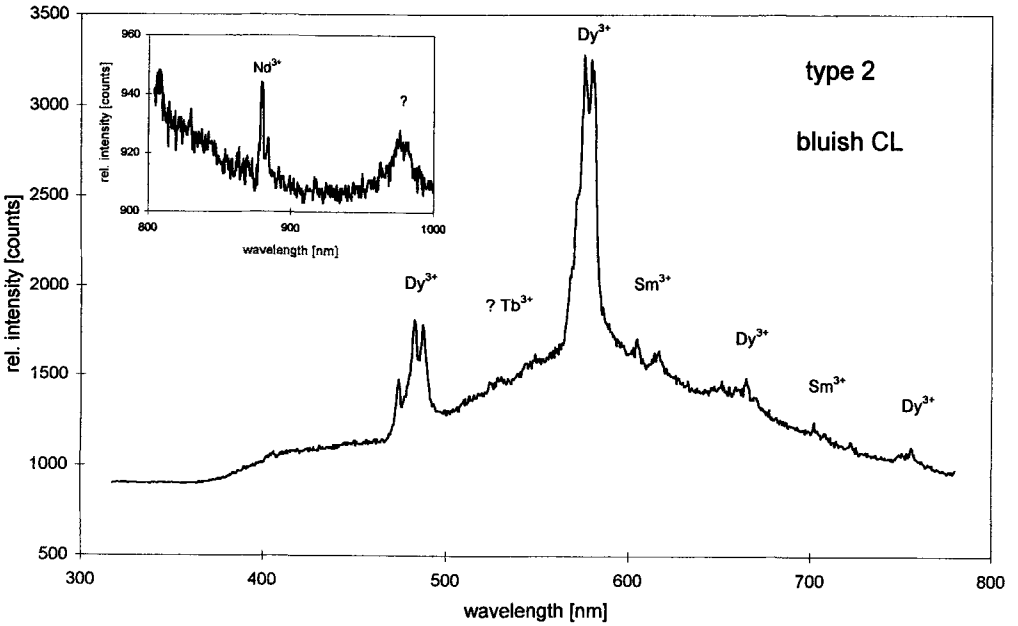

FIG. 4. CL spectrum of a bluish luminescing zircon grain (type 2 - see Plate 7B) with dominant sharp Dy^{3+} emission peaks and weak emissions activated by Sm^{3+}, Tb^{3+} and Nd^{3+}.

(triplet) are due to the $^4F_{9/2}$ $^6H_{15/2}$ transitions within the Dy^{3+} ions and the multiplet near 580 nm corresponds to the $^4F_{9/2}$ $^6H_{13/2}$ electron transitions (Marfunin, 1979). These results are consistent with investigations on doped synthetic zircon crystals (Cesbron *et al.*, 1993).

Although Dy^{3+} is common in the blue luminescing zircons it does not primarily cause the blue CL colour. On the contrary, a negative correlation between the Y and Dy concentration and the intensity of the blue CL colour was observed in natural zircons (Remond *et al.*, 1992; Hoffmann and Long, 1984). Investigations of synthetic zircons doped by Dy show a greenish-yellow CL colour (Cesbron *et al.*, 1993). The blue CL is mainly caused by an intrinsic emission band centered near 430 nm. Iacconi and Caruba (1980) and Remond *et al.* (1992) concluded that this blue emission band probably results from bond breaking of the $[SiO_4]^{4-}$ groups by incident electron beam. Recent results indicate that the emission around 430 nm is more likely related to electron defects on the $[SiO_4]$ groups (Kempe *et al.*, 1998).

Yellow CL is due to a broad emission band between 500 and 700 nm (Fig. 6). According to Nicholas (1967) this broad band is associated with lattice defects resulting from the radioactive decay of trace uranium. Similar results were reported by Remond *et al.* (1992) from U,Th-containing synthetic zircons with an emission band near 580 nm. A similar emission is observed in natural quartz which can probably be related to oxygen vacancies in the SiO_4 tetrahedra (Krbetschek *et al.*, 1998). It is well known that radiation can lead to the creation of such intrinsic vacancies in solids. However, the intensity of the yellow emission does not correlate with the U and Th concentration of the zircons investigated (compare Table 1). The dull bluish luminescing rim of type 1 zircon has the highest U content but shows no significant yellow emission band. Thus, the U content alone cannot cause the intense yellow emission in zircons. Cathodoluminescence might be expected to correlate with the radiation dose of the sample, which could be independent of the U concentration. On the other hand, other factors such as trace impurities have to be discussed too. Considering that Yb, a common trace element in zircon, may also induce a CL emission band, it is uncertain whether the yellow CL in zircon is caused by electron defects localized on the $[SiO_4]$ groups or activation by Yb^{2+} generated by radiation (Kempe *et al.*, 1998).

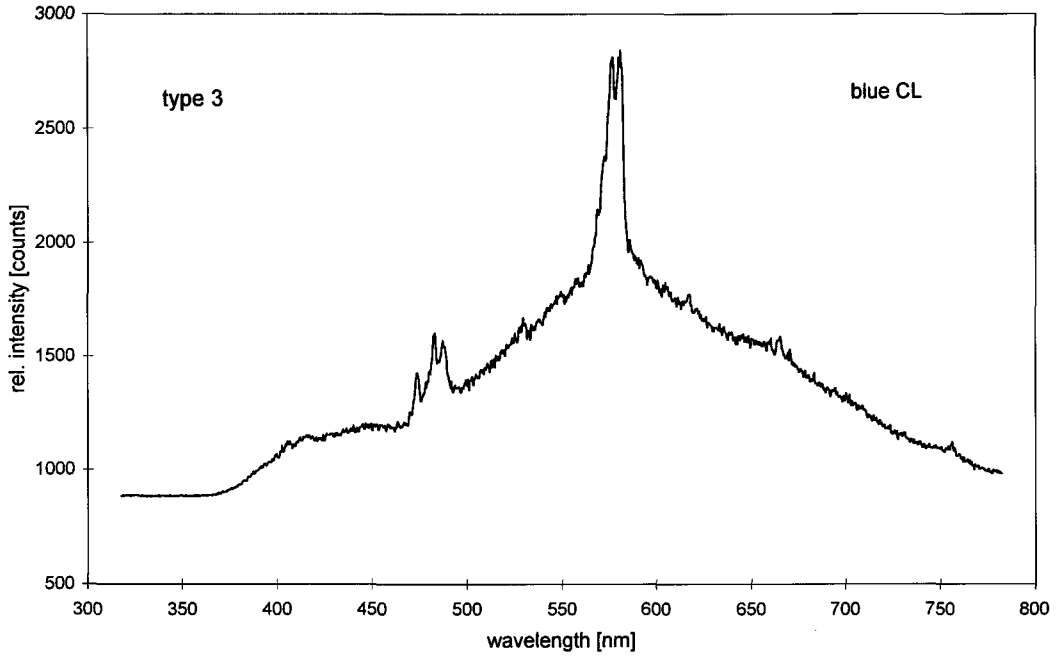

FIG. 5. CL spectrum of a blue luminescing type 3 zircon (see Plate 7C).

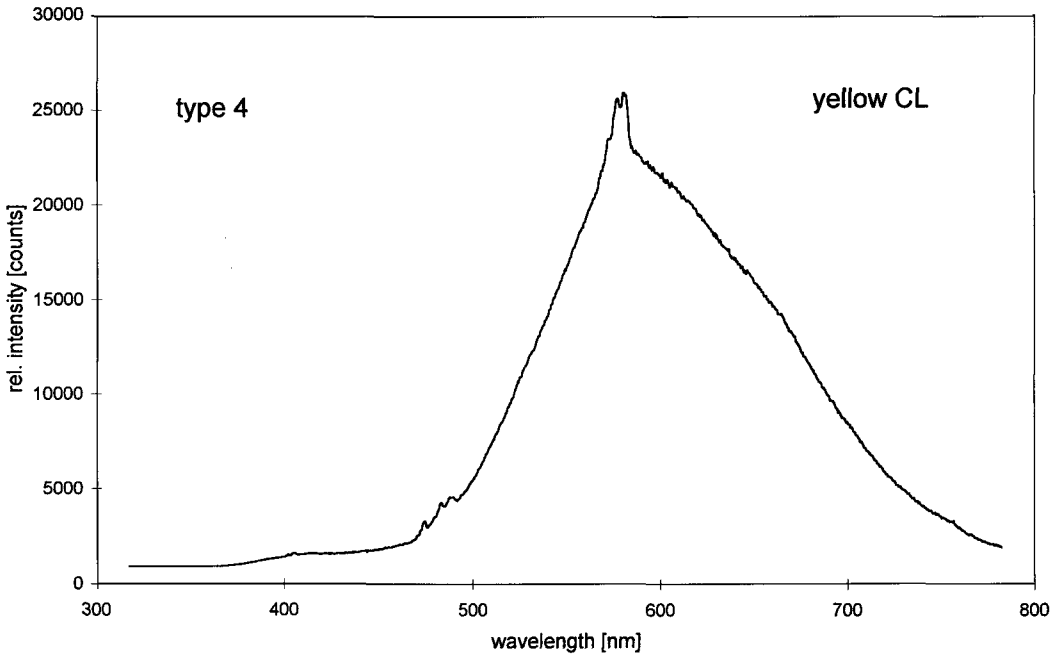

FIG. 6. CL spectrum of a yellow luminescing zircon belongig to type 4 (see Plate 7D) with a broad emission band between 500 and 700 nm.

TABLE 1. Results of SHRIMP measurements on detrital zircon grains

Zircon	Spot	$^{206}Pb/^{238}U$	$^{207}Pb/^{235}U$	$^{207}Pb/^{206}Pb$	U [ppm]	Th [ppm]	U/Th
type 1	a (core)	0.40878 ± 0.00346	7.72840 ± 0.10944	0.13710 ± 0.00141	103	112	0.9
type 1	b (core)	0.37887 ± 0.00339	7.00683 ± 0.20545	0.13413 ± 0.00359	103	130	0.8
type 1	c (core)	0.33142 ± 0.00256	6.07196 ± 0.08592	0.13303 ± 0.00145	97	86	1.1
type 1	d (core)	0.35145 ± 0.00271	6.62482 ± 0.09132	0.13671 ± 0.00143	128	150	0.9
type 1	e (rim)	0.06324 ± 0.00044	0.48475 ± 0.01302	0.05559 ± 0.00139	903	3	301.0
type 1	f (rim)	0.06396 ± 0.00045	0.49173 ± 0.01765	0.05575 ± 0.00191	572	2	286.0
type 1	g (rim)	0.06268 ± 0.00044	0.47413 ± 0.01285	0.05485 ± 0.00138	723	2	361.5
type 1	h (rim)	0.06105 ± 0.00037	0.43077 ± 0.01167	0.05177 ± 0.00131	643	2	321.5
type 1	i (rim)	0.05910 ± 0.00037	0.45594 ± 0.01658	0.05595 ± 0.00196	879	3	293.0
type 2	k	0.05430 ± 0.00042	0.39267 ± 0.02557	0.05244 ± 0.00334	268	204	1.3
type 3	l	0.07144 ± 0.00052	0.52249 ± 0.02248	0.05304 ± 0.00220	644	193	2.8
type 4	m	0.31321 ± 0.00224	4.60046 ± 0.03991	0.10652 ± 0.00043	546	153	3.6

Despite the uncertain origin of the yellow CL band, it can be concluded that variations of the integral SEM-CL intensity are mainly controlled by the intensities of the broad bands and the Dy^{3+} peaks. Thus, internal structures revealed by CL are due to variations in defect density (lattice defects and trace element incorporation) within the zircon grains.

To decide whether the four different zircon types evaluated by CL really represent different origins, ion probe (SHRIMP) analyses on the single zircon grains were carried out which provide *in situ* high resolution U-Pb dating (Table 1). Our measurements show that the U-Pb ages of the zircons from Weferlingen scatter over a wide range (340 to 1750 Ma, see Fig. 7).

The type 1 zircon inherits different ages of core and rim (inset of Fig. 7) which indicates reworking of pre-existing Precambrian zircons during Early Devonian (probably metamorphic origin). The differences between core and rim are also emphasized by the strongly differing U and Th concentrations (see Table 1). The type 2 zircon represents Variscan age (about 340 Ma) and the zircon of type 3 plots somewhat below 450 Ma. The age of the zircon belonging to type 4 was determined at about 1750 Ma. These results emphasize the different origin of the different zircon types backing up earlier conclusions that the quartz sand from Weferlingen is quite heterogeneous in terms of provenance. Götze (1995) postulated at least three possible provenance areas of the sand: (1) Triassic sediments in the vicinity of the Allertal graben, (2) volcanic rocks of the Flechtingen ridge, and (3) metamorphic source rocks probably from Southern Scandinavia. Unfortunately, the lack of available data from detailed zircon investigations of possible source rocks prevents a more detailed provenance discussion. Nevertheless, the results demonstrate that zircons preserve the CL properties inherited from the primary source rocks, although the zircons may have undergone several geological processes and sedimentary cycles which very differently influenced shape and roundness of the grains. Using these characteristic properties a differentiation of zircons with different geological history and age is possible.

These results illustrate that a successful U-Pb chronology requires a careful characterization and preselection of the zircon grains to be analysed. This is especially true in sediments where detrital zircons can be of unknown and multiple origin. Besides morphological criteria, the use of sophisticated analytical methods especially CL microscopy, SEM-CL and BSE imaging allows zircon populations to be distinguished and to reveal internal structures relevant for dating. However, a reliable age distribution statistics for serious provenance interpretation requires more analyses than realized in this case study. The U-Pb ages determined by SHRIMP in this study are only relevant to emphasize that the zircon types distinguished really represent different origins.

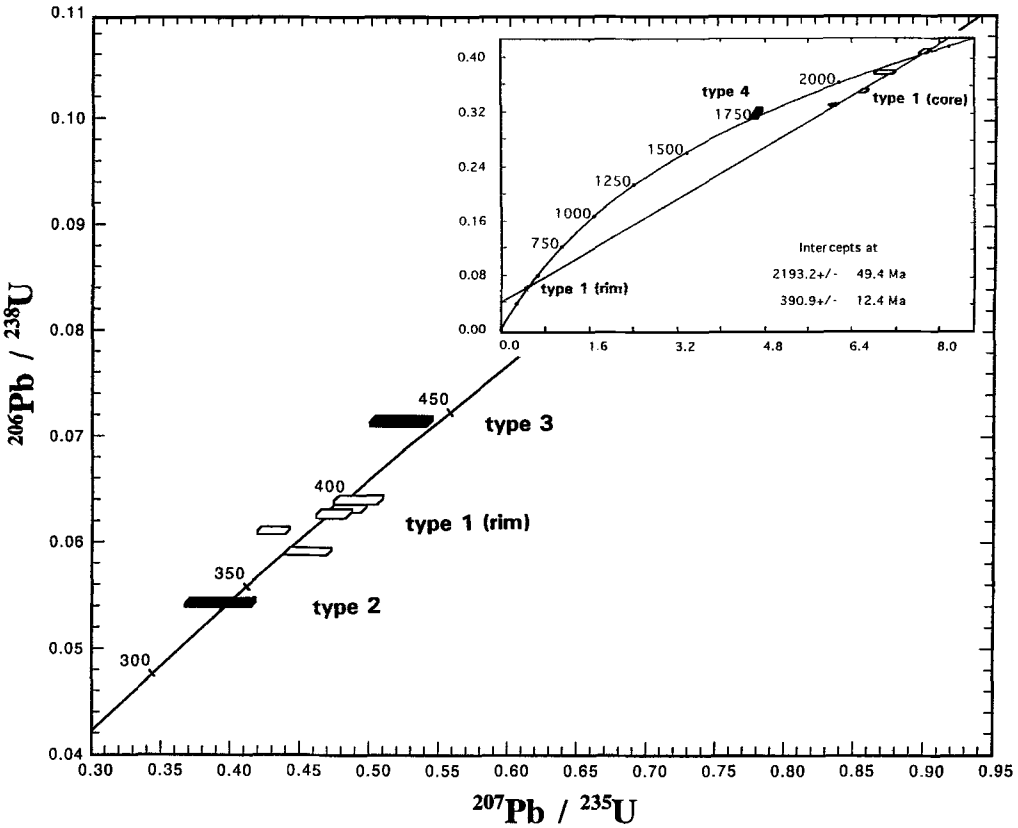

FIG. 7. U-Pb concordia plot of the analysed detrital zircon grains showing the age between 300 and 450 Ma and on the inset between 300 and 2300 Ma, respectively.

Conclusions

In the present case study optical and spectral cathodoluminescence combined with SHRIMP ion probe measurements were successfully used to distinguish and characterize detrital zircon populations in the Cretaceous Weferlingen quartz sand. The results show that different zircon types distinguished by internal structures and cathodoluminescence characteristics (colour, spectra) have different U-Pb ages reaching from 340 to 1750 Ma and thus, represent different geological histories. The results give an indication of a heterogeneous provenance of the sediment. Although the number of zircons analysed is too limited to get reliable age distribution statistics, the advantages of the combined use of sophisticated analytical methods are demonstrated.

Acknowledgements

An earlier version of this paper was improved from critical reviews by A. Finch and an anonymous reviewer.

References

Cesbron, F., Ohnenstetter, D., Blanc, P., Rouer, O. and Sichere, M.-C. (1993) Incorporation de terres rares dans zircons de synthèse: étude par cathodoluminescence. *C. R. Acad. Sci. Paris*, **316**, série II, 1231–8.

Compston, W., Williams, I.S. and Meyer, C. (1984) U-Pb geochronology of zircons from lunar breccia 73217 using a sensitive high mass-resolution ion microprobe. *J. Geophys. Res.*, **89**, B525–34.

Götze, J. (1995) Genetic information of accessory

minerals in clastic sediments. *Zbl. Geol. Paläont.*, Teil I, H **1/2**, 101–18.

Götze, J. (1997) Mineralogy and geochemistry of German high-purity quartz sands. In *Mineral Deposits: Research and Exploration* (H. Papunen, ed.). Balkema, Rotterdam Brookfield, 721–4.

Hoffmann, J.F. and Long, J.V.P. (1984) Unusual sector zoning in Lewisian zircons. *Mineral. Mag.*, **48**, 513–7.

Iacconi, P., Deville, A. and Gaillard, B. (1980) Trapping and emission centres in X-irradiated zircon. (II): Contribution of the SiO_4^{4-} groups. *Phys. Stat. Sol. (a)*, **59**, 639–46.

Jaffey, A.H., Flynn, K.F., Glendenin, L.E., Bentley, W.C. and Essling, A.M. (1971) Precision measurement of the half-lives and specific activities of U235 and U238. *Phys. Rev. C*, **4**, 1889–907.

Kempe, U., Gruner, T., Nasdala, L. and Wolf, D. (1998) Relevance of cathodoluminescence for interpretation of U-Pb zircon ages (with an example of application to a study of zircons from the Saxonian Granulite Complex, Germany). In *Cathodoluminescence in Geosciences* (M. Pagel *et al.*, eds). Springer Verlag (in the press).

Krbetschek, M.R., Götze, J., Dietrich, A. and Trautmann, T. (1998) Spectral information from minerals relevant for luminescence dating. *Radiat. Measurements*, **27**, 695–748.

Marfunin, A.S. (1979) *Spectroscopy, Luminescence and Radiation Centers in Minerals*. Springer Verlag, Berlin, 352 p.

Neuser, R.D., Bruhn, F., Götze, J., Habermann, D. and Richter, D.K. (1995) Cathodoluminescence: Method and application. *Zbl. Geol. Paläont.*, Teil I, H **1/2**, 287–306.

Nicholas, J.V. (1967) Origin of the luminescence in natural zircon. *Nature*, **215**, 1476.

Pidgeon, R.T., Furfaro, D., Kennedy, A.K., Nemchin, A.A. and van Bronswijk, W. (1994) Calibration of zircon standards for the Curtin SHRIMP II. In: 8th Conf. Geochronol. Cosmochronol. Isotope Geol., Berkeley, *U.S. Geol. Surv. Circular*, **1107**, 251.

Remond, G., Cesbron, F., Chapoulie, R., Ohnenstetter, D., Roques-Carmes, C. and Schvoerer, M. (1992) Cathodoluminescence applied to the microcharacterization of mineral materials: a present status in experimentation and interpretation. *Scanning Microscopy*, **6**, 23–68.

Smith, J.B., Barley, M.E., Groves, D.I., Krapez, B., McNaughton, N.J., Bickle, M.J. and Chapman, H.J. (1998) The Sholl Shear Zone, West Pilbara: evidence for a domain boundary structure from integrated tectonostratigraphic analyses, SHRIMP U-Pb dating and isotopic and geochemical data of granitoids. *Precamb. Res.*, **88**, 143–71.

[*Manuscript received 27 September 1998*]

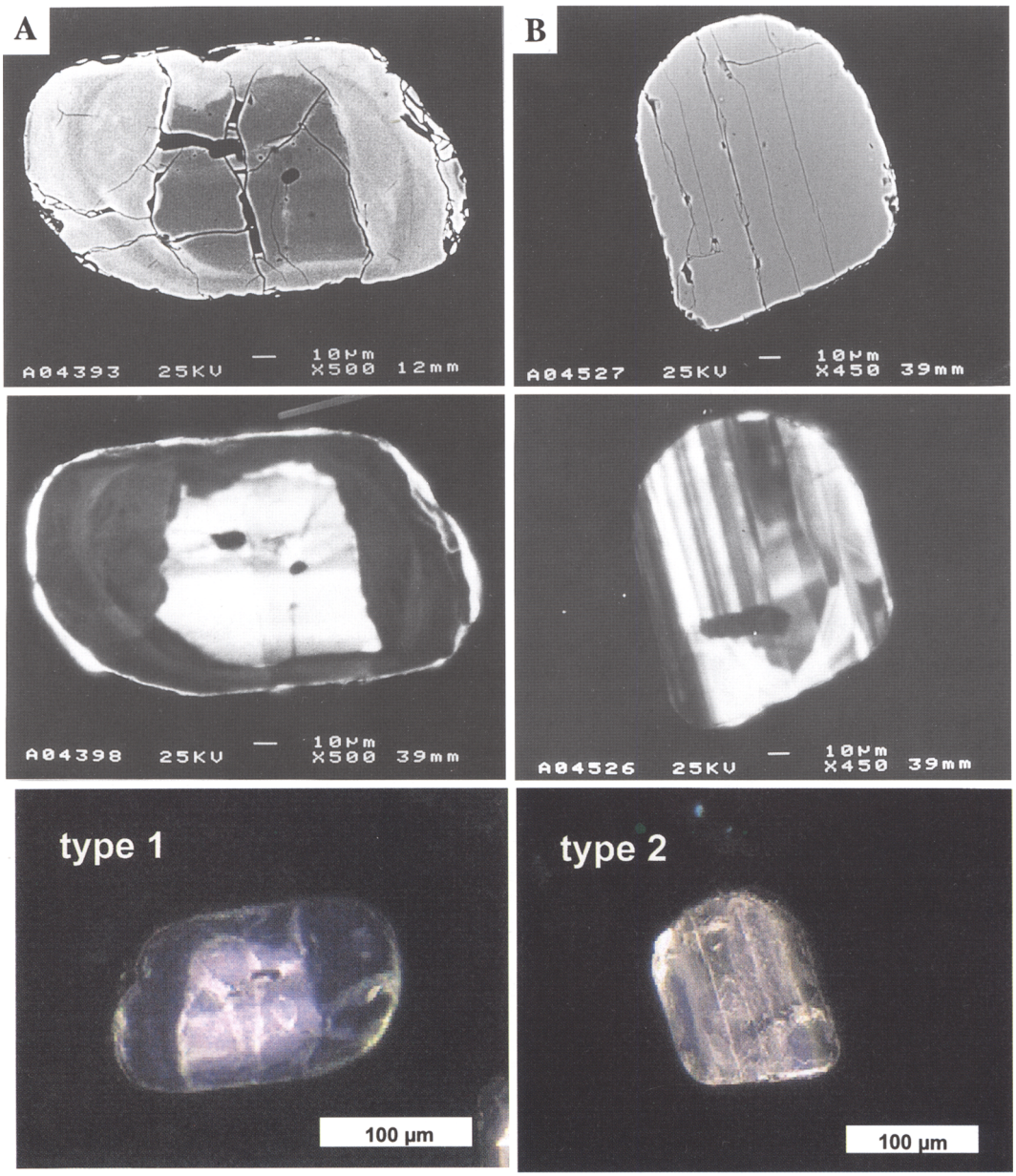

PLATE 7. BSE, SEM-CL and CL-microscope images of four zircon types occuring in the Weferlingen quartz sand. [(i) this page] (A) type 1: appearently weakly zoned, rounded grains with relict cores; (B) type 2: well rounded fragments of optically more or less homogeneous zircon grains showing CL zoning predominantly parallel to the *z*-axis. [(ii) opposite page] (C) type 3: idiomorphic to slightly rounded zircon grains typically showing oscillatory concentric blue CL zoning; (D) type 4: well-rounded zircon fragments with bright-yellow CL.

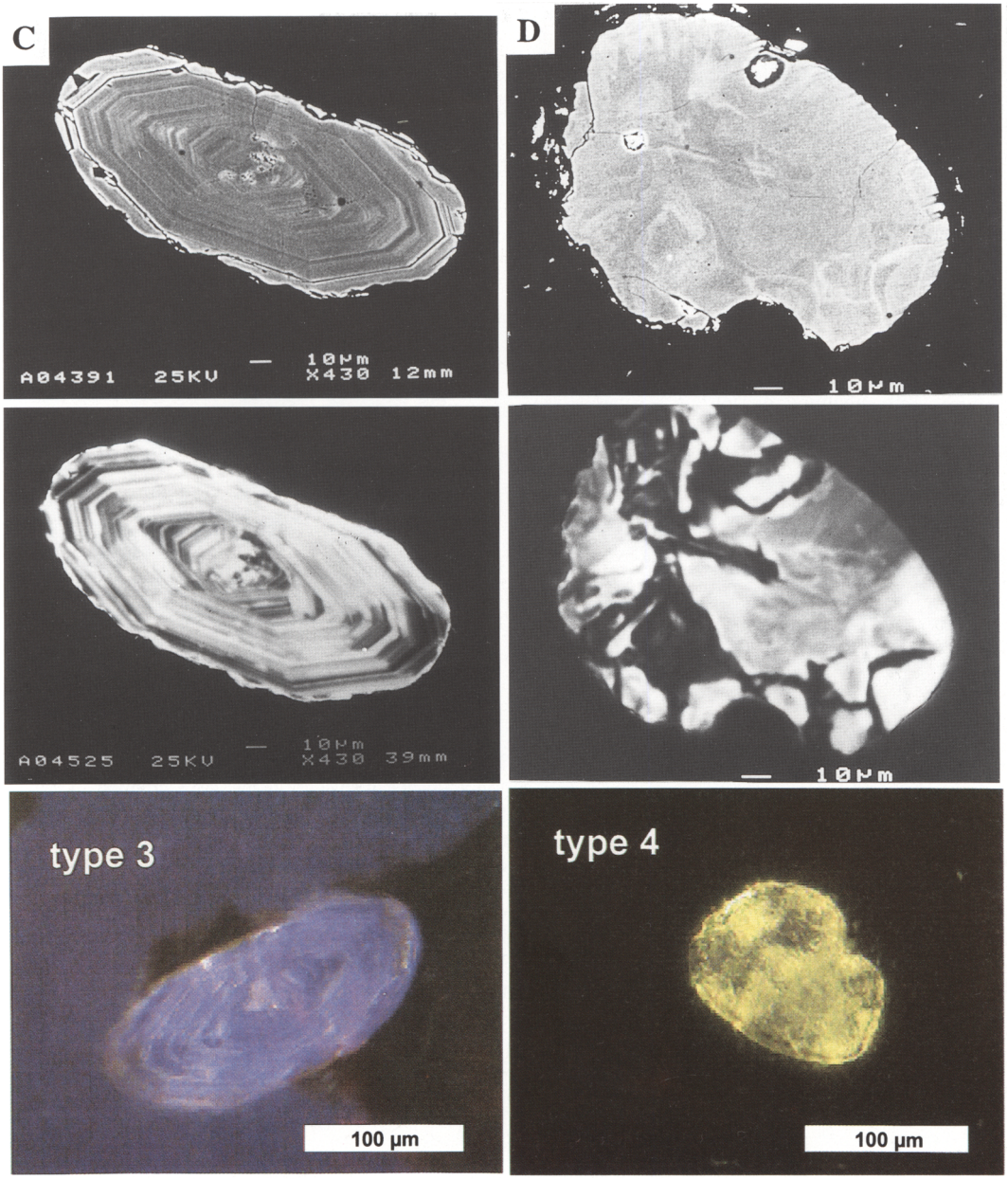
C
A04391 25KV 10µm X430 12mm
D
10µm
A04525 25KV 10µm X430 39mm
10µm
type 3
100 µm
type 4
100 µm